

SUPPLEMENTARY MATERIALS AND METHODS

Antibodies.

The antibodies used in western blots are listed below

Antibodies	Company
p38 MAPK14, p38 MAPK14-T180-82, IGF1R- β , IR- β , pIGF1R-T980, Cyclin-D1, pPI3K-110 α , PTEN, β -actin, Notch4, IRS-1, AKT, VEGFR2, IGFBP-2, Tuberin, Bax, Tau, pMAPK-T202/204, pSRC-Y416, SRC, Beclin, pAKT-S473, pcMET-Y1235, pAKT-T308, EEF2K, AMPK- α , PRAS40, pYB-1-S102, pmTOR-S244-48, pS6-S235/236, pS6-S240/244, p70S6K-T389, Gab2, Bad, Rictor, Raptor, MEK-1/2, pFOXO3a-S318/321, eIF4E, pEIF4E-S209 and pSTAT3-Y705	Cell Signaling Technologies
FLI1, HER3, and PI3K-85	Santa Cruz Biotechnology
RNA helicase A, SMAD-3, c-Kit, DHFR, and CD-239, pIGF-1R-Y1131, Smad3, pSmad-S423-425	Abcam
Stat3	Santa Cruz
PKC α , pPKC-S657, PARK7-DJ-1, and p-Her2(Y1248)	EMD Millipore
Wnt-8 β and ADAM-8	LS Biosciences

Proteins analyzed in RPPA panels

#	Official Ab Name	Ab Name Reported on Dataset	Gene Name	Company
1	14-3-3 beta	14-3-3-beta	YWHAB	Santa Cruz
2	14-3-3 epsilon	14-3-3-epsilon	YWHAE	Santa Cruz
3	14-3-3 zeta	14-3-3-zeta	YWHAZ	Santa Cruz
4	4E-BP1	4E-BP1	EIF4EBP1	CST
5	4E-BP1_pS65	4E-BP1_pS65	EIF4EBP1	CST
6	4E-BP1_pT37_T46	4E-BP1_pT37_T46	EIF4EBP1	CST
7	53BP1	53BP1	TP53BP1	CST
8	Acetyl CoA Carboxylase 1	ACC1	ACACA	Epitomics
9	Acetyl-CoA Carboxylase_pS79	ACC_pS79	ACACA ACACB	CST
10	ACVRL1	ACVRL1	ACVRL1	Abcam
11	ADAR1	ADAR1	ADAR	Abcam
12	Akt	Akt	AKT1 AKT2 AKT3	CST
13	Akt_pS473	Akt_pS473	AKT1 AKT2 AKT3	CST
14	Akt_pT308	Akt_pT308	AKT1 AKT2 AKT3	CST
15	AMPK α	AMPK-alpha	PRKAA1	CST
16	AMPK α _pT172	AMPK-alpha_pT172	PRKAA1	CST
17	Androgen Receptor	AR	AR	Epitomics
18	Annexin I	Annexin-I	ANXA1	BD Biosciences
19	Annexin VII	Annexin-VII	ANXA7	BD Biosciences

#	Official Ab Name	Ab Name Reported on Dataset	Gene Name	Company
20	A-Raf	A-Raf	ARAF	CST
21	ARHI	ARHI	DIRAS3	MDACC Laboratory
22	ATM	ATM	ATM	CST
23	ATM_pS1981	ATM_pS1981	ATM	CST
24	ATP5H	ATP5H	ATP5H	Abcam
25	ATR	ATR	ATR	CST
26	Bad_pS112	Bad_pS112	BAD	CST
27	Bak	Bak	BAK1	Epitomics
28	BAP1	BAP1	BAP1	Santa Cruz
29	Bax	Bax	BAX	CST
30	BCL2	Bcl2	BCL2	Dako
31	Bcl-xL	Bcl-xL	BCL2L1	CST
32	Beclin	Beclin	BECN1	Santa Cruz
33	beta-Catenin	b-Catenin	CTNNB1	CST
34	beta-Catenin_pT41_S45	b-Catenin_pT41_S45	CTNNB1	CST
35	Bid	Bid	BID	Abcam
36	Bim	Bim	BCL2L11	Abcam
37	B-Raf	B-Raf	BRAF	Santa Cruz
38	B-Raf_pS445	B-Raf_pS445	BRAF	CST
39	BRCA2	BRCA2	BRCA2	CST
40	Caspase-7 cleavedD198	Caspase-7-cleaved	CASP7	CST
41	Caspase-8	Caspase-8	CASP8	CST
42	Caveolin-1	Caveolin-1	CAV1	CST
43	CD29	CD29	ITGB1	BD Biosciences
44	CD31	CD31	PECAM1	Dako
45	CD49b	CD49b	ITGA2	BD Biosciences
46	cdc2/CDK1	CDK1	CDC2- CDK1	CST
47	CDKN2A/p16INK4a	p16INK4a	CDKN2A	Abcam
48	Chk1	Chk1	CHEK1	CST
49	Chk1_pS345	Chk1_pS345	CHEK1	CST
50	Chk2	Chk2	CHEK2	CST
51	Chk2_pT68	Chk2_pT68	CHEK2	CST
52	c-Jun_pS73	c-Jun_pS73	JUN	CST
53	c-Kit	c-Kit	KIT	Abcam
54	Claudin 7	Claudin-7	CLDN7	Novus Biologicals
55	c-Met	c-Met	MET	CST
56	c-Met_pY1234_Y1235	c-Met_pY1234_Y1235	MET	CST
57	c-Myc	c-Myc	MYC	Santa Cruz
58	COL6A1	Collagen-VI	COL6A1	Santa Cruz
59	Complex II Subunit	Complex-II-Subunit	SDHA	Invitrogen
60	Cox IV	Cox-IV	COX4I1	Abcam
61	Cox2	Cox2	PTGS2	CST
62	C-Raf/Raf-1	C-Raf	RAF1	Millipore
63	C-Raf_pS338	C-Raf_pS338	RAF1	CST
64	Cyclin B1	Cyclin-B1	CCNB1	Epitomics
65	Cyclin D1	Cyclin-D1	CCND1	Santa Cruz
66	Cyclin E1	Cyclin-E1	CCNE1	Santa Cruz
67	Cyclophilin F	Cyclophilin-F	PPIF	Abcam

#	Official Ab Name	Ab Name Reported on Dataset	Gene Name	Company
68	Dvl3	Dvl3	DVL3	CST
69	E2F-1	E2F1	E2F1	Santa Cruz
70	E-Cadherin	E-Cadherin	CDH1	CST
71	eEF2	eEF2	EEF2	CST
72	eEF2K	eEF2K	EEF2K	CST
73	EGFR	EGFR	EGFR	CST
74	EGFR pY1068	EGFR pY1068	EGFR	CST
75	EGFR pY1173	EGFR pY1173	EGFR	Abcam
76	eIF4E	eIF4E	EIF4E	CST
77	eIF4G	eIF4G	EIF4G1	CST
78	ER alpha pS118	ER-alpha pS118	ESR1	Epitomics
79	ErbB2/HER2	HER2	ERBB2	Lab Vision
80	ErbB2/HER2 pY1248	HER2 pY1248	ERBB2	R&D Systems
81	ErbB3/HER3	HER3	ERBB3	Santa Cruz
82	ErbB3/HER3 pY1289	HER3 pY1289	ERBB3	CST
83	ERCC1	ERCC1	ERCC1	Santa Cruz
84	ERRFI1/MIG6	MIG6	ERRFI1	Sigma-Aldrich
85	Estrogen Receptor	ER-alpha	ESR1	Lab Vision
86	Ets-1	Ets-1	ETS1	Bethyl
87	FAK	FAK	PTK2	CST
88	FAK pY397	FAK pY397	PTK2	CST
89	Fatty Acid Synthase	FASN	FASN	CST
90	Fibronectin	Fibronectin	FN1	Epitomics
91	FoxM1	FoxM1	FOXO3	CST
92	FoxO3a	FoxO3a	FOXO3	CST
93	FoxO3a pS318_S321	FoxO3a pS318_S321	FOXO3	CST
94	G6PD	G6PD	G6PD	Santa Cruz
95	Gab2	Gab2	GAB2	CST
96	GAPDH	GAPDH	GAPDH	Life Technologies
97	GATA3	GATA3	GATA3	BD Biosciences
98	GCN5L2	GCN5L2	KAT2A	CST
99	Glycogen Synthase	Gys	GYS1	CST
100	Glycogen Synthase pS641	Gys_pS641	GYS1	CST
101	GPBB	GPBB	PYGB	Novus Biologicals
102	GSK-3alpha/beta	GSK-3ab	GSK3A GSK3B	Santa Cruz
103	GSK-3alpha/beta pS21_S9	GSK-3ab_pS21_S9	GSK3A GSK3B	CST
104	GSK-3beta pS9	GSK-3b_pS9	GSK3B	CST
105	Heregulin	Heregulin	NRG1	CST
106	HIAP	HIAP	BIRC2	Millipore
107	Histone H3	Histone-H3	H3F3A H3F3B	Abcam
108	IGF-1Receptor beta	IGF1R-beta	IGF1R	CST
109	IGFBP2	IGFBP2	IGFBP2	CST
110	INPP4b	INPP4b	INPP4B	CST
111	IRS1	IRS1	IRS1	Millipore
112	JAB1	JAB1	COPS5	Santa Cruz
113	JNK/SAPK pT183_Y185	JNK pT183_Y185	MAPK8	CST
114	JNK2	JNK2	MAPK9	CST

#	Official Ab Name	Ab Name Reported on Dataset	Gene Name	Company
115	KMT3A/HYPB/HIF 1	SETD2	SETD2	Abcam
116	Lck	Lck	LCK	CST
117	MAPK_pT202_Y204	MAPK_pT202_Y204	MAPK1 MAPK3	CST
118	Mcl 1	Mcl-1	MCL1	CST
119	MDM2_pS166	MDM2_pS166	MDM2	CST
120	MEK1	MEK1	MAP2K1	Epitomics
121	MEK1_pS217_S221	MEK1_pS217_S221	MAP2K1 MAP2K2	CST
122	MEK2	MEK2	MAP2K2	CST
123	Merlin/NF2	Merlin	NF2	Novus Biologicals
124	MSH2	MSH2	MSH2	CST
125	MSH6	MSH6	MSH6	Novus Biologicals
126	mTOR	mTOR	MTOR	CST
127	mTOR_pS2448	mTOR_pS2448	MTOR	CST
128	Myosin heavy chain 11	Myosin-11	MYH11	Novus Biologicals
129	Myosin IIa_pS1943	Myosin-IIa_pS1943	MYH9	CST
130	NAPSIN A	NAPSIN-A	NAPSA	Abcam
131	N-Cadherin	N-Cadherin	CDH2	CST
132	NDRG1_pT346	NDRG1_pT346	NDRG1	CST
133	NF-kappaB p65_pS536	NF-kB-p65_pS536	RELA	CST
134	Notch1	Notch1	NOTCH1	CST
135	N-Ras	N-Ras	NRAS	Santa Cruz
136	p21	p21	CDKN1A	Santa Cruz
137	p27 KIP 1	p27-Kip-1	CDKN1B	Abcam
138	p27 KIP 1_pT198	p27_pT198	CDKN1B	Abcam
139	p27/Kip1_pT157	p27_pT157	CDKN1B	R&D Systems
140	p38 alpha MAPK	p38-alpha	MAPK14	CST
141	p38 MAPK	p38	MAPK14	CST
142	p38 MAPK_pT180_Y182	p38_pT180_Y182	MAPK14	CST
143	p53	p53	TP53	CST
144	p70 S6 Kinase_pT389	p70-S6K_pT389	RPS6KB1	CST
145	p70/S6K1	p70-S6K1	RPS6KB1	Epitomics
146	PAI-1	PAI-1	SERPINE1	BD Biosciences
147	PARK7/DJ1	DJ1	PARK7	Abcam
148	PARP cleavedD214	PARP-cleaved	PARP1	CST
149	PARP-1	PARP1	PARP1	Santa Cruz
150	Paxillin	Paxillin	PXN	Epitomics
151	PCNA	PCNA	PCNA	Abcam
152	Pcdcd-1L1	Pcdcd-1L1	CD274	Santa Cruz
153	Pcdcd4	Pcdcd4	PDCD4	Rockland
154	PDGFR beta	PDGFR-beta	PDGFRB	CST
155	PDK1	PDK1	PDPK1	CST

#	Official Ab Name	Ab Name Reported on Dataset	Gene Name	Company
156	PDK1_pS241	PDK1_pS241	PDPK1	CST
157	PEA-15	PEA-15	PEA15	CST
158	PED/PEA-15_pS116	PEA-15_pS116	PEA15	Invitrogen
159	PI3 Kinase p110 alpha	PI3K-p110-alpha	PIK3CA	CST
160	PI3K p85	PI3K-p85	PIK3R1	Millipore
161	PKC alpha	PKC-alpha	PRKCA	Millipore
162	PKC alpha_pS657	PKC-alpha_pS657	PRKCA	Millipore
163	PKC beta II_pS660	PKC-beta-II_pS660	PRKCA PRKCB PRKCD PRKCE PRKCH PRKCQ	CST
164	PKC delta_pS664	PKC-delta_pS664	PRKCD	Millipore
165	PMS2	PMS2	PMS2	Novus Biologicals
166	PRAS40_pT246	PRAS40_pT246	AKT1S1	Life Technologies
167	PREX1	PREX1	PREX1	Abcam
168	Progesterone Receptor	PR	PGR	Abcam
169	PTEN	PTEN	PTEN	CST
170	Rab11	Rab11	RAB11A RAB11B	CST
171	Rab25	Rab25	RAB25	CST
172	Rad50	Rad50	RAD50	Millipore
173	Rad51	Rad51	RAD51	CST
174	Raptor	Raptor	RPTOR	CST
175	Rb	Rb	RB1	CST
176	Rb_pS807_S811	Rb_pS807_S811	RB1	CST
177	RBM15	RBM15	RBM15	Novus Biologicals
178	Rictor	Rictor	RICTOR	CST
179	Rictor_pT1135	Rictor_pT1135	RICTOR	CST
180	RSK	RSK	RPS6KA1 RPS6KA2 RPS6KA3	CST
181	S6_pS235_S236	S6_pS235_S236	RPS6	CST
182	S6_pS240_S244	S6_pS240_S244	RPS6	CST
183	SCD	SCD	SCD	Santa Cruz
184	SF2/ASF	SF2	SRSF1	Invitrogen
185	Shc_pY317	Shc_pY317	SHC1	CST
186	Smac/Diablo	Smac	DIABLO	CST
187	Smad1	Smad1	SMAD1	Epitomics
188	Smad3	Smad3	SMAD3	Abcam
189	Smad4	Smad4	SMAD4	Santa Cruz
190	Snail	Snail	SNAI1	CST
191	Src	Src	SRC	Millipore

#	Official Ab Name	Ab Name Reported on Dataset	Gene Name	Company
192	Src Family_pY416	Src_pY416	SRC LYN FYN LCK YES1 HCK	CST
193	Src_pY527	Src_pY527	SRC YES1 FYN FGR	CST
194	Stat3_pY705	Stat3_pY705	STAT3	CST
195	Stat5a	Stat5a	STAT5A	Abcam
196	Stathmin 1	Stathmin-1	STMN1	Abcam
197	Syk	Syk	SYK	Santa Cruz
198	TAZ	TAZ	WWTR1	CST
199	TIGAR	TIGAR	C12ORF5	Abcam
200	Transferrin Receptor	TFRC	TFRC	Novus Biologicals
201	Transglutaminase II	Transglutaminase	TGM2	Lab Vision
202	TSC1/Hamartin	TSC1	TSC1	CST
203	TSC2 Tuberin_pT1462	Tuberin_pT1462	TSC2	CST
204	TTF1	TTF1	NKX2-1	Abcam
205	Tuberin	Tuberin	TSC2	Epitomics
206	Twist	TWIST	TWIST2	Santa Cruz
207	Tyro3	Tyro3	TYRO3	CST
208	UBAC1	UBAC1	UBAC1	Sigma-Aldrich
209	UGT1A	UGT1A	UGT1A1	Santa Cruz
210	UQCRC2	UQCRC2	UQCRC2	Abcam
211	VDAC1/Porin	Porin	VDAC1	Abcam
212	VEGF Receptor 2	VEGFR-2	KDR	CST
213	VHL	VHL	VHL	BD Biosciences
214	XRCC1	XRCC1	XRCC1	CST
215	YAP	YAP	YAP1	Santa Cruz
216	YAP_pS127	YAP_pS127	YAP1	CST
217	YB1	YB1	YBX1	Novus Biologicals
218	YB1_pS102	YB1_pS102	YBX1	CST

Cell lines

ES cell lines A4573, TC32 and TC71 were maintained in RPMI 1640 medium (Mediatech; Manassas, VA) containing 10% (vol/vol) fetal bovine serum (Gemini Bio-

Products; Sacramento, CA) and antibiotics (100 IU/ml penicillin and 100 mg/ml streptomycin [Mediatech]) in a humidified incubator at 37°C in a 5% CO₂ atmosphere.

Preparation of drug stock solutions

For in vivo applications, the primary stock solution of ridaforolimus (10 mg/ml. Merck; Kenilworth, NJ) was prepared in N,N-dimethyl acetamide and stored at -80°C. The working concentrations of ridaforolimus were prepared as needed by diluting the stock solution (10%) in vehicle comprising 10% Tween 80, 40% polyethylene glycol-400, and 40% sterile water. The primary stock solution of dalotuzumab was supplied by Merck at a concentration of 20.16 mg/ml in vehicle containing 20 mM L-histidine, 150 mM NaCl, and 0.5% (w:w) polysorbate 80 (pH 6). The working concentrations of dalotuzumab were prepared in the same formulation buffer. The primary stock solution of CGP57380 (150 mg/ml. Seleckchem; Houston, TX) for in vivo applications was prepared in N,N-dimethyl acetamide and stored at -80°C. The working concentrations of CGP57380 (1.2 mgX5 per week in IP injection) were prepared as needed by diluting the stock solution (10%) in vehicle comprising 10% Tween 80, 40% polyethylene glycol-400, and 40% sterile water. The primary stock solution of alpelisib (Novartis, 15 mg/ml) for in vivo applications was prepared in 0.5% carboxymethylcellulose sodium salt and stored at -80°C. The working concentrations of alpelisib were 1.5 mg/dose (5 days per week) in oral gavage. For in vitro applications, ridaforolimus (5.05 mM), OSI-906 (Seleckchem; 11.86 mM), dasatinib (Seleckchem; 10 mM), CGP57380 (Seleckchem; 10 mM), WP1722 (10mM. Produced in the lab of Dr. Waldemar Priebe. MDACC; Houston,

TX) and NVP-ADW-742 (Seleckchem; 11.02 mM) stock solutions were prepared in dimethyl sulfoxide (DMSO) and stored at -20°C.

Generation of ES clones with acquired drug resistance

TC32 and TC71 ES clones with acquired resistance to OSI-906, NVP-ADW-742, or ridaforolimus were generated by maintaining the corresponding parental cell lines with increasing concentrations of the agents (up to 2.3 μM for OSI-906, 1.5 μM for NVP-ADW-742, and 50 μM for ridaforolimus) for 7 months. All parental and acquired drug resistant cell lines were tested twice per year for mycoplasma contamination using the MycoAlert Detection Kit (Lonza Group Ltd.; Allendale, NJ) according to the manufacturer's protocol and validated using short-tandem repeat fingerprinting with an AmpFLSTR Identifier kit as previously described[39].

Assessment of cell viability (colorimetric methods and flow cytometry).

Cell viability was measured using a colorimetric assay as previously described, using the following drug concentrations: 0.0004-15 μM for OSI-906 and NVP-ADW-742; 0.003-200 μM for ridaforolimus; 0.3125-40 μM for dasatinib; and 1.25-40 μM for CGP57380)[39]. IC_{50} values from three replicated experiments were calculated by performing sigmoidal dose-response curve fitting using the Graph-Pad Prism version 6.0 software program. The apoptosis and proliferation of drug-resistant ES clones were indirectly assessed using Annexin V/propidium iodide staining and Ki67 intracellular labeling, respectively[39]. Cytometry data were acquired using a FACSCanto II flow

cytometer (BD Biosciences; San Jose, CA) and analyzed using the FlowJo version 10.0.6 software program (Tree Star; Ashland, OR).

In vitro assessment of cell line drug resistance

Colony formation assays were used to assess cells' drug resistance. Drug-sensitive ES cells and drug-resistant ES clones in media were seeded in 6-well plates at 200 cells/well. After 24 hours, the cells were treated with the indicated concentrations of the drugs and then allowed to grow in media for 2 weeks. The cell colonies were then fixed with methanol, stained with crystal violet, and counted manually.

In vitro siRNA-based assays

Short interfering RNAs (siRNAs) targeting human protein kinase C alpha (PKC- α) and a non-specific universal negative control were obtained from Sigma-Aldrich (St Louis, MO). siRNAs were validated by assessing their protein expression with Western blotting as previously described[39]. Reverse transfections in 96-well plates were carried out using 40-nM siRNA with HiPerFect Transfection Reagent (Qiagen; Valencia, CA) in OptiMEM I Reduced Serum Medium (Life Technologies; Carlsbad, CA) according to the manufacturer's protocol. The adherently growing ES cells were cultivated for 24 hours after reverse transfection and then treated with fresh RPMI complete medium containing the indicated drugs in serial diluted concentrations for up to 72 hours. The effect of siRNA knockdown on the cells' drug resistance was assessed using the CellTiter-Blue cell viability assay (Promega; Madison, WI) according to the manufacturer's protocol.

Plates were read on a DTX 880 Multimode Detector microplate reader (Beckman Coulter; Indianapolis, IN).

Proteomic studies (western blots and reverse-phase protein arrays)

The preparation of extracted proteins from cells or tumors for western blotting and reverse-phase protein lysate array (RPPA) analysis were prepared as described previously[33]. Western blotting and detection was performed using previously described methods[39]. Antibodies used are summarized in the supplemental Experimental Procedures. An RPPA analysis of drug-sensitive ES cells and drug-resistant ES clones or of EW5 and TC71 xenografts treated with dalotuzumab and/or ridaforolimus or control vehicle were performed simultaneously using the same array. Lysates were processed, spotted onto nitrocellulose-coated FAST slides, probed with 183 validated primary antibodies, and detected using earlier methods [39]. MicroVigene software program (VigeneTech) was used for automated spot identification, background correction, and individual spot-intensity determination. Expression data was normalized for possible unequal protein loading, taking into account the signal intensity for each sample for all antibodies tested. Log_2 values were media-centered by protein to account for variability in signal intensity by time and were calculated using the formula $\text{log}_2 \text{ signal} - \text{log}_2 \text{ median}$.

Generation of EW5 and TC71 ES xenografts and evaluation of dalotuzumab and/or ridaforolimus

Male NOD (SCID)-IL-2Rg^{null} mice (The Jackson Laboratory; Farmington, CT) were subcutaneously injected with TC71 cells (10^6 cells/animal) or received EW5 explants (2 mm) to generate xenografts. All mice were maintained under barrier conditions and treated using protocols approved by The University of Texas MD Anderson Cancer Center's Institutional Animal Care and Use Committee (eACUF Protocol #03-11-02532) and Institutional Biosafety Committee (eIBC #HA0411-346-1).

Once their tumors reached a volume of 150 mm^3 , 6-9 mice per group received ridaforolimus (5 mg/kg daily, 5 times per week) and/or dalotuzumab (0.5 mg intraperitoneally twice weekly) or a placebo control (sterile vehicle buffer). Tumor volumes were measured using digital calipers at study initiation and 2–5 times per week thereafter for up to 35 days (TC71 xenografts), 73 days (EW5 xenografts), or until their tumors reached 1500 mm^3 , whichever came first. Of the 50 mice used in the experiments, three (5.7%; one in the ridaforolimus group and two in the ridaforolimus plus dalotuzumab) died within the first week of treatment, before their tumors reached 1500 mm^3 , likely because of the high volume of diluted ridaforolimus given ($300 \mu\text{l/day}$). A Kaplan-Meier analysis was performed to assess drug efficacy. Statistical analyses between control and treated group or between different treated groups were performed with the log-rank (Mantel-Cox) test using Graph-Pad Prism 6.0 and are summarized in the Supplementary table 1.

Gene expression profiling and analysis

Total RNA was extracted from EW5 xenograft tumors using the miRNeasy Mini Kit (Qiagen). RNA quality was assessed, and RNA was assigned an integrity number, before amplification and labeling using the GeneChip 3' IVT Express Kit (Affymetrix; Santa Clara, CA). Amplified and biotinylated cRNAs were hybridized onto Affymetrix GeneChip Human Genome U133A 2.0 cartridge arrays, then washed and stained per the manufacturer's instructions. Arrays were scanned using a GeneChip Scanner 3000 system, and the initial raw data were extracted using the GeneChip Command Console-Expression software (Affymetrix). The CEL files and extracted raw data were quantified using a robust multiarray analysis algorithm and normalized using median centering. EW5 xenograft-bearing mice treated with dalotuzumab or normotonic saline solution (control), were subjected to this genomic profiling and a t-test was used to assess differences between the two treatment groups. Unsupervised double hierarchical clustering used a Pearson correlation distance metric and Ward's linkage clustering method to separate six samples into two groups based upon expression of genes or expressed sequence tags (EST). Array data for dalotuzumab-treated and control EW5 xenografts (GSE67529) are available from the Gene Expression Omnibus repository.

Combination experiments and determination of synergy

An IC_{50} isobologram analysis was performed using previously described methods to examine the dose dependent interaction between OSI-906 and dasatinib or between ridaforolimus and CGP57380 drug combinations on ES cell line sensitivity[39]. Drug synergy was determined using CalcuSyn software 2.1 (Biosoft; Cambridge, UK), which

analyzes the data from WST-1 proliferation assays to determine the interaction between equipotent drug combinations as compared to the concentration of single drug.

Immunohistochemical staining of relapsed ES patients tumor to IGF-1R/mTOR therapy

Samples were obtained from patients undergoing surgical tumor resection under an institutional review board-approved protocol (# LAB08-0151) through the UT-MD-Anderson cancer center. All the patients provided written informed consent prior to surgical resection. Immunohistochemical staining was performed on formalin-fixed and paraffin-embedded (FFPE) tumor patient sections after deparaffinization, antigen retrieval and blockade of endogenous peroxidase activity and total proteins. The primary antibodies diluted in the blocking buffers were added overnight at 4°C for pIGF-1R (Abcam; Cambridge, MD), IGF-1R (Santa Cruz), pSTAT3 (Cell Signaling; Danvers, MD), STAT3 (Santa Cruz), pEIF4E (Santa Cruz), eIF4E (Cell Signaling), pSMAD3 (Abcam), pPKC (Abcam), PKC (Abcam), pSRC (Cell Signaling), SRC (Cell Signaling) and SMAD3 (Abcam). Sequentially, slides were washed and incubated with the secondary antibody EnVision Dual Link (DAKO; Carpinteria, CA). Slides were then developed with 3,3'-diaminobenzidine tetrahydrochloride substrate that includes horseradish peroxidase enzyme and hematoxylin was used for counter staining. Staining was evaluated and scored by HMA. Photomicrographs were captured using a Nikon Microphot FXA microscope (Nikon Instruments; Melville, NJ), an Olympus DP70 camera (Olympus America; Jupiter, FL), and the QCapture Suite PLUS software (QImaging; Surrey, British Columbia, CA).

Statistical analyses

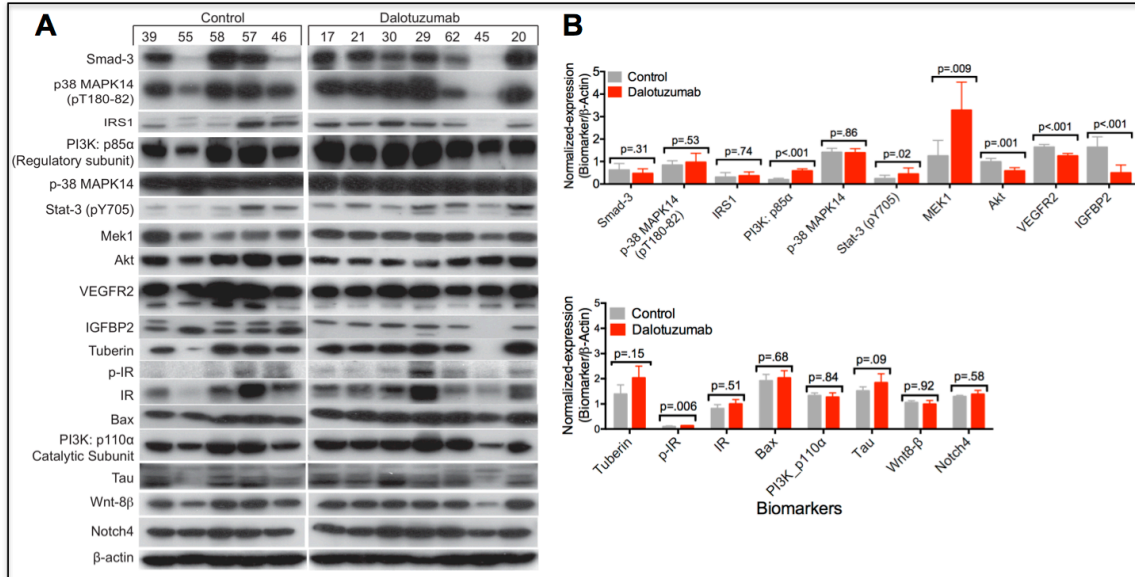
RPPA and gene expression profiling data were median-centered. Principal component analysis was used to check for a batch effect and feature-by-feature two-sample t-tests were used to assess differences between treatment and control groups. We also used feature-by-feature one-way analysis of variance (ANOVA) followed by the Tukey test to perform pair comparisons for all groups. Beta-uniform mixture models were used to fit the resulting p value distributions to adjust for multiple comparisons. The cutoff p values and number of significant proteins were computed for several different false discovery rates (FDRs).

Biostatistical analyses comparing two groups were performed using an unpaired t-test with Gaussian distribution followed by the Welch correction. To distinguish between treatment groups, we used one-way ANOVA with the Geisser-Greenhouse correction. Differences with p values <0.05 were considered significant. Within clustered image maps (CIM), unsupervised double hierarchical clustering used the Pearson correlation distance and Ward's linkage method as the clustering algorithm to link entities (proteins or genes) and samples.

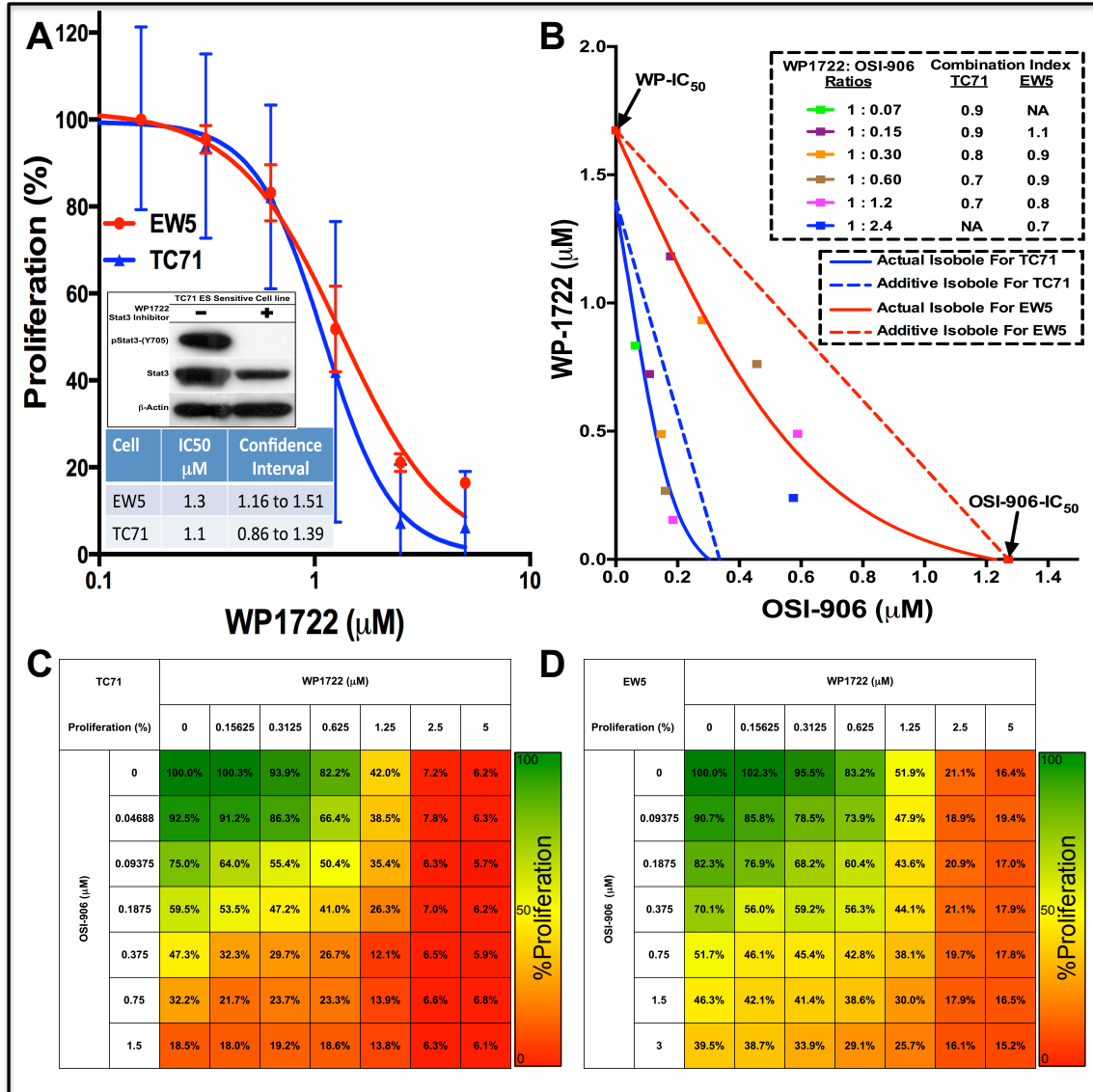
Supplementary Table 1. Therapeutic enhancement of dalotuzumab and ridaforolimus in Ewing sarcoma xenografts

XENOGRAFT	TUMOR GROWTH DELAY (DAYS) & *P-VALUE (TREATMENT VS. CONTROL)			*P-VALUE TREATMENT VS. TREATMENT			THERAPEUTIC ENHANCEMENT
	Dalotuzumab	Ridaforolimus	Combination	Combination Vs. Ridaforolimus	Combination Vs. Dalotuzumab	Dalotuzumab Vs. Ridaforolimus	
EW5	16 p=.02	13 p=.06	Not Reached p=.009	p=.02	p=.02	p=.55	Yes
TC71	1 p=.31	5.5 p=.01	30 p=.005	p=.006	p=.005	p=.02	Yes

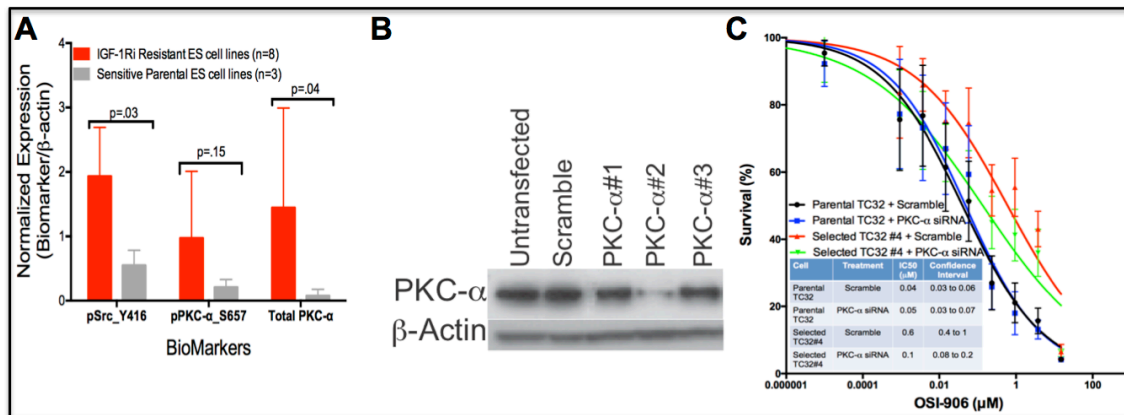
* p values were obtained using the log-rank (Mantel-Cox) test.



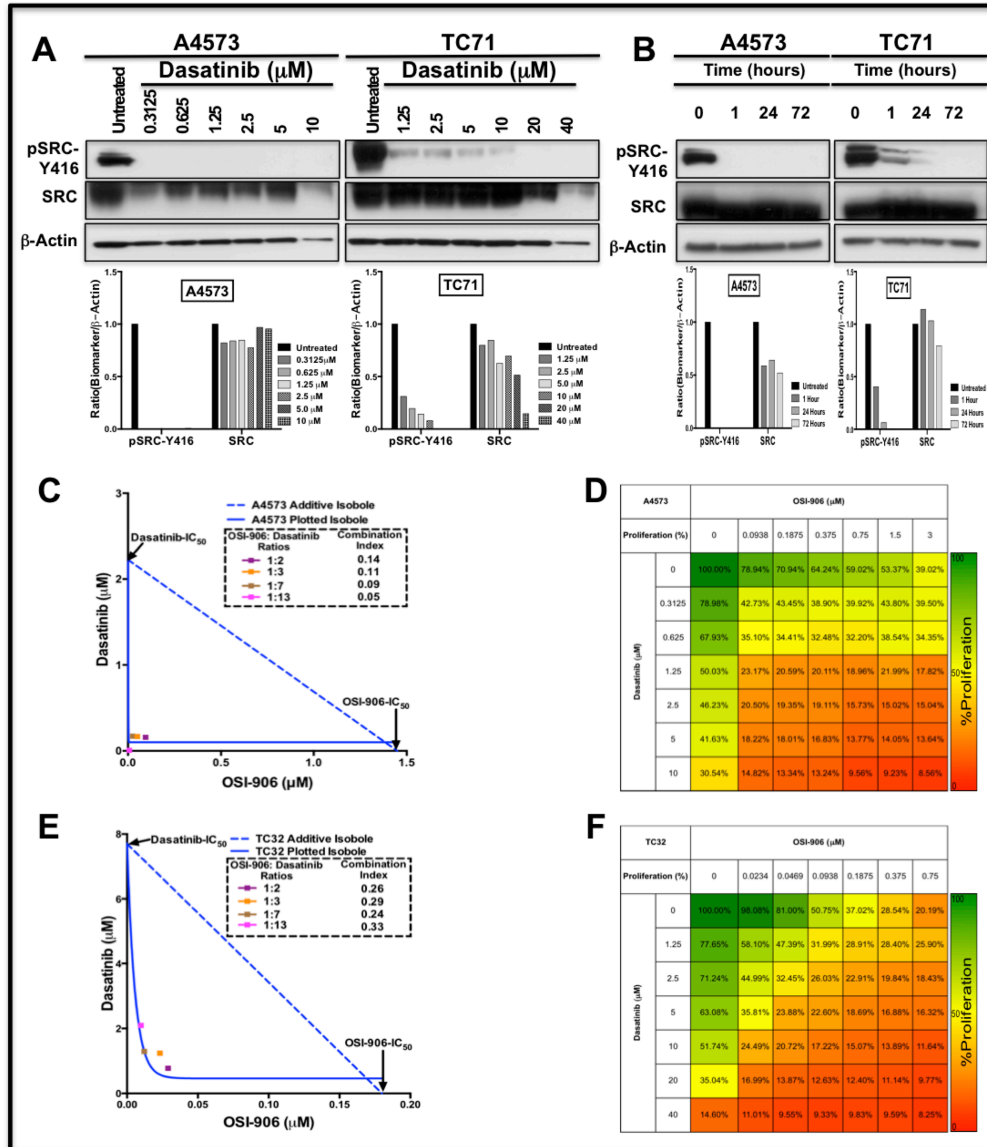
Supplementary Figure 1. MOR and cell signaling analyses following dalotuzumab treatment in ES xenografts. (A) Western blot validation of proteins differentially identified by RPPA in Figure 2D within dalotuzumab-treated (n=7) and control (n=5) xenografts. **(B)** Normalized protein expressions relative to β -actin in dalotuzumab-treated and control xenografts with their respective p-value using unpaired two-tailed Student test statistical analyses; bars show mean \pm SD. MOR = mechanism of resistance



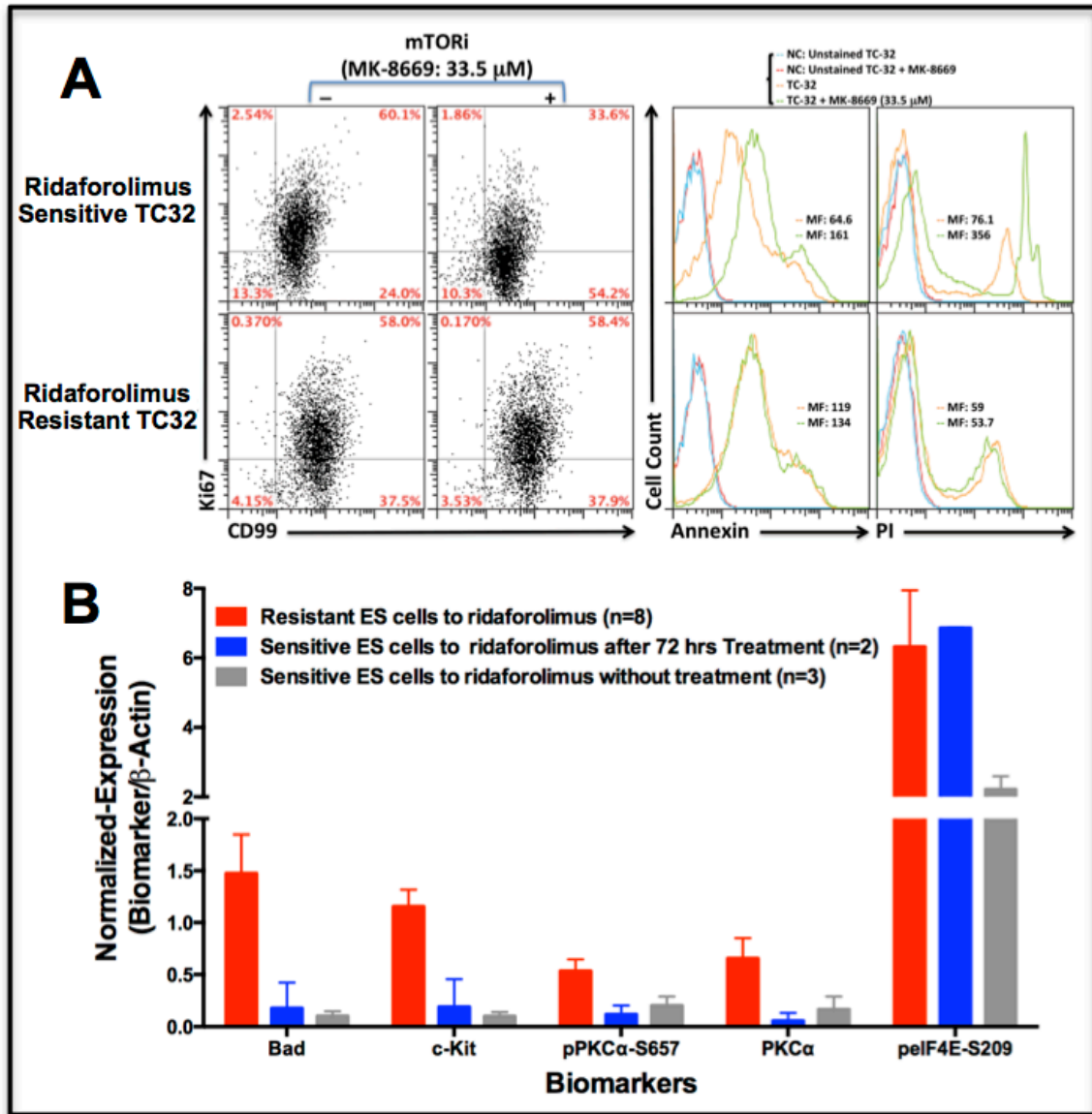
Supplementary Figure 2. Isobologram analysis of the combination IGF-1R/IR and stat3 inhibition on in vitro EW5 and TC71 ES cell proliferation. (A) In vitro Cell proliferation based-assay after 72 hours of exposure to stat3 inhibitor, WP-1722 in ES cell lines. The IC₅₀ values of each EW5 and TC71 drug-sensitive parental ES cell lines and pStat3-Y705/Stat3/b-actin protein expression levels in ES TC71 cell line are also shown; bars show mean ± SD. (B) Isobologram analysis showed that OSI-906 and WP1722 are synergistic in their ability to inhibit EW5 and TC71 cell proliferation. The diagonal, dotted line indicated additivity extrapolated from single agent IC₅₀ doses of OSI-906 or WP1722 and the solid curve with colored symbols shows dose requirements at different WP1722:OSI-906 ratios to achieve 50% inhibition of EW5 and TC71 ES cell proliferation. Combination index (CI) values are given for each ratio. (C&D) Dose response effect of OSI-906 and/or WP-1722 in the TC71 (C) and EW5 (D) ES cell proliferation. Each data point in panels C&D is the mean of three replicates from three different experiments. Each data point in C and D are the mean of nine replicates from three different experiments.



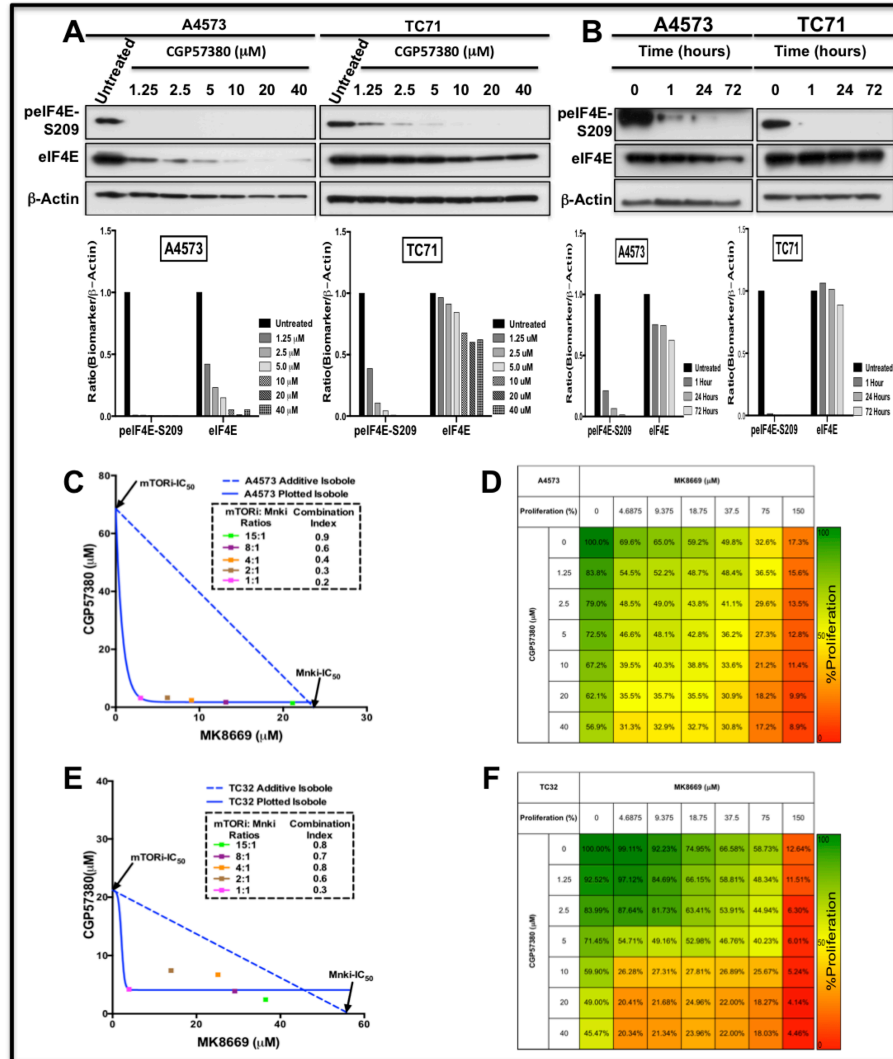
Supplemental Figure 3. Combination effect of IGF-1R/IR and PKC- α blockades on in vitro ES cell survival. (A) Western blot validation of proteins differentially identified by RPPA in Figure 4A between resistant and sensitive ES cell lines to IGF-1R blockade after β -actin normalization. Respective p-value using unpaired two-tailed Student test statistical analyses are also shown; bars show mean \pm SD. (B) Western blot of PKC- α and β -Actin expression in parental TC32 ES cell line (untransfected, transfected with PKC- α siRNA gene silencer sequences (PKC- α #1-3), and siRNA with nonsense/scrambled negative sequence). (C) Cell proliferation assay: OSI-906-sensitive parental cells and OSI-906-resistant clones were transiently transfected with PKC- α #2 siRNA (capable of knocking down the PKC- α expression) for 72 hours. Cell survival was assessed using the CellTiter-Blue assay. Curves represent the mean values of nine replicates from three different experiments, and bars represent standard deviations. The OSI-906 IC₅₀ values for each drug-sensitive parental cell line and selected drug-resistant cell lines, along with the associated confidence intervals, are also shown; bars show mean \pm SD. ES = Ewing sarcoma; pSrc_Y416 = phospho-Sarc tyrosine kinase; PKC- α = protein kinase C alpha; IC₅₀ = half maximal inhibitory concentration; IGF-1Ri = Insulin-like growth factor 1 receptor inhibition, siRNA = small interfering RNA.



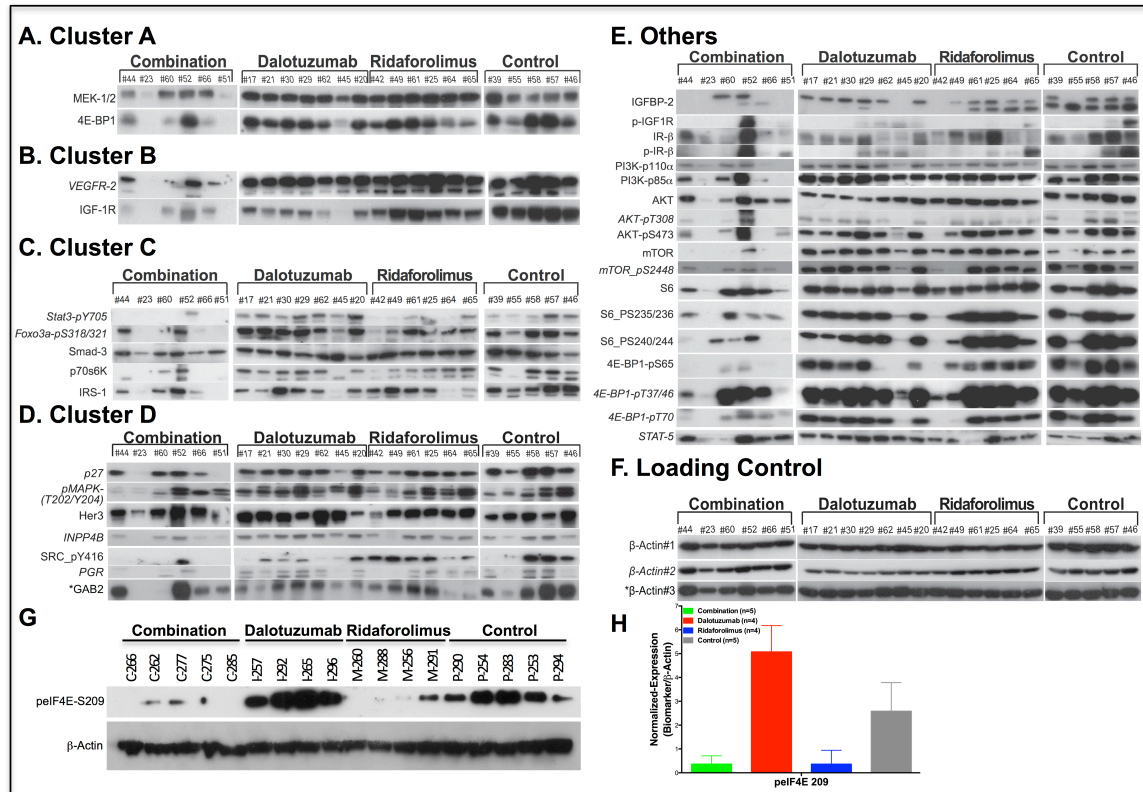
Supplementary Figure 4. In vitro combination of IGF-1R/IR and Src blockade on ES cell survival. Western blots showed inhibition of pSrc-Y416 and total Src expression by dasatinib in dose (A) and time (B) dependent manner (3 μM of dasatinib) in A4573 and TC71 ES cell lines (C&E, respectively). Isobologram analysis indicates that OSI-906 and dasatinib synergistically inhibit A4573 and TC32 ES cell line proliferation. The diagonal, dotted line indicates additivity extrapolated from single agent IC₅₀ doses of OSI-906 or dasatinib and the solid curve with colored symbols shows dose requirements at different OSI-906:Dasatinib ratios necessary to achieve 50% inhibition of A4573 and TC32 ES cell proliferation. Combination index (CI) values are given for each ratio, with synergism <1, additivity =1, and antagonism >1. (D&F) Dose response effect of OSI-906 and/or dasatinib in the A4573 and TC32 ES cell proliferation. Each data point in panels C-F is the mean of nine replicates from three different experiments. IGF-1R = Insulin-like growth factor 1 receptor; IR = insulin receptor; Src, Src tyrosine kinase; ES = Ewing sarcoma; IC₅₀ = half maximal inhibitory concentration.



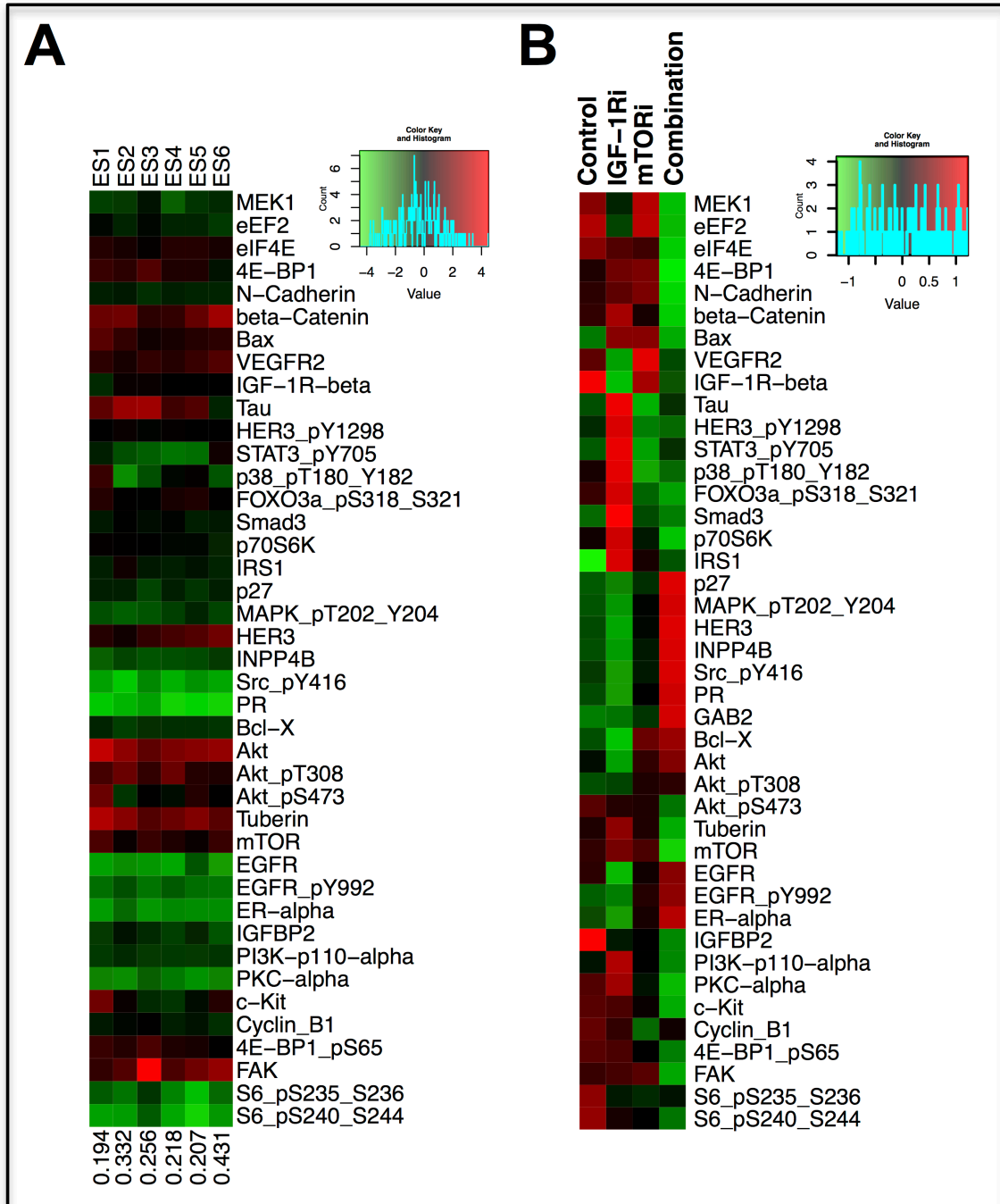
Supplementary Figure 5. Characterization of mTORi-resistant ES cells. (A) Seventy-two hours after MK-8669 treatment (33.5 μ M), using Ki67 labelling, propidium iodide and Annexin V staining, and flow cytometry. (B) Western blot validation of proteins differentially identified by RPPA in Figure 5A after β -actin normalization; bars show mean \pm SD. ES = Ewing sarcoma; mTORi = mammalian target of rapamycin inhibition; Ki67 = antigen that is a nuclear protein associated with cellular proliferation; CD99 = Cluster of differentiation 99; NC = negative control; MF = mean fluorescence; Bad = Bcl-2-associated death promoter; c-Kit = tyrosine-protein kinase Kit (CD117); PKC α = protein kinase C alpha; pelf4E-S209 = phospho eukaryotic translation initiation factor 4E.



Supplementary Figure 6. In vitro combination of mTOR and Mnk blockade on ES cell proliferation. Western blot analyses of pEIF4E-S209, total EIF4E and β -Actin expression after in vitro CGP57380 (Mnk inhibitor) treatment in dose (A) and time (B) dependent manner of A4573 (15 μ M of CGP57380) and TC71 (10 μ M of CGP57380) ES cell lines; normalized EIF4E and pEIF4E-S209 protein expression is relative to β -Actin. (C&E) Isobologram analysis showed that ridaforolimus (MK-8669) and CGP57380 are synergistic in their ability to inhibit A4573 and TC32 cell proliferation. The diagonal, dotted line indicates additivity extrapolated from single agent IC_{50} doses of ridaforolimus or CGP57380 and the solid curve with colored symbols shows dose requirements at different ridaforolimus:CGP57380 ratios to achieve 50% inhibition of A4573 and TC32 ES cell proliferation. Combination index (CI) values are given for each ratio, with synergism <1 , additivity $=1$, and antagonism >1 . (D&F) Dose response effect of ridaforolimus and/or CGP57380 in the A4573 and TC32 ES cell proliferation. Each data point in panels D&F is the mean of nine replicates from three different experiments. mTORi = mammalian target of rapamycin inhibition; Mnk = MAPK interacting protein kinase inhibition; EIF4E-S209 = eukaryotic translation initiation factor 4E.



Supplementary Figure 7. (A-F) Western blot validation of proteins identified by RPPA in Figure 6B. (G) peIF4E-S209 and β -Actin protein expressions in treated xenografts presented in Figure 1C. (H) Normalized peIF4E-S209 protein relative to β -actin in treated xenografts shown in Figure 1C; bars show mean \pm SD. Abbreviated gene of the indicated protein is provided in the supplementary table of proteins analyzed in RPPA.



Supplementary Figure 8. RPPA profiling of pretreated ES patient tumors (**A**) and averaged EW5 xenografts treated mice (**B**). The Pearson correlation coefficients between the pretreated patient tumors and the averaged xenograft control group are provided in the bottom of the figure 8A. Abbreviated gene of the indicated protein is provided in the supplementary table of proteins analyzed in RPPA.